

Mapping of soil moisture by time domain reflectometry and electrical resistivity tomography at Velika Gorica well field, Zagreb aquifer

Bačani, Laura; Posavec, Kristijan; Šumanovac, Franjo; Kapuralić, Josipa

Source / Izvornik: **Geofizika**, 2022, 39, 281 - 296

Journal article, Published version

Rad u časopisu, Objavljena verzija rada (izdavačev PDF)

<https://doi.org/10.15233/gfz.2022.39.13>

Permanent link / Trajna poveznica: <https://um.nsk.hr/um:nbn:hr:169:270519>

Rights / Prava: [Attribution-NonCommercial 4.0 International](#)/[Imenovanje-Nekomercijalno 4.0 međunarodna](#)

Download date / Datum preuzimanja: **2025-02-05**



Repository / Repozitorij:

[Faculty of Mining, Geology and Petroleum Engineering Repository, University of Zagreb](#)



DOI: <https://doi.org/10.15233/gfz.2022.39.13>
Original scientific paper



Mapping of soil moisture by time domain reflectometry and electrical resistivity tomography at Velika Gorica well field, Zagreb aquifer

Laura Bačani[✉], Kristijan Posavec[✉], Franjo Šumanovac[✉]
and Josipa Kapuralić[✉]

Faculty of Mining, Geology and Petroleum Engineering, University of Zagreb, Zagreb, Croatia

Received 15 December 2021, in final form 4 July 2022

Knowing the soil moisture distribution in the unsaturated zone can improve understanding the water flow through the unsaturated zone and thereby enable the calculation of aquifer recharge, which occurs through precipitation. One part of the Zagreb aquifer recharge occurs through infiltration from precipitation. In order to observe and model infiltration from precipitation through the unsaturated zone, the research polygon was constructed at the Velika Gorica well field, located in the southern part of the Zagreb aquifer, Croatia, where hourly measurements of electric conductivity (EC) and soil moisture content were carried out. EC and soil moisture data are measured by Time Domain Reflectometry (TDR) probes which are placed at different depths in the unsaturated zone. Furthermore, electrical resistivity tomography (ERT) measurements were conducted. Geophysical data, along with moisture and EC data from TDR probes, were used as input data for MoisturEC software, in order to obtain soil moisture distribution along a 2D profile. MoisturEC program offers three options for translating EC data to moisture content data which are all tested in this research. We obtained eight moisture content distributions along the observed profile and concluded that MoisturEC provides reasonable results with input data from geophysical measurements and TDR probe measurements. Soil moisture distribution in the unsaturated zone represents the initial conditions for further unsaturated flow modeling. Understanding the flow in the unsaturated zone enables the quantification of effective infiltration and can improve groundwater management.

Keywords: unsaturated zone, soil moisture content, Time Domain Reflectometry (TDR), electrical resistivity, Zagreb aquifer, MoisturEC program

1. Introduction

Groundwater reserves of the Zagreb aquifer represent the only source of potable water for the inhabitants of the City of Zagreb and Zagreb County. In past decades, groundwater level decline has been identified in the Zagreb aquifer

(Vujević and Posavec, 2018). Consequently, it became important to understand and quantify the recharge mechanisms for the proper and sustainable management of this natural resource. According to Posavec (2006), recharge of the Zagreb aquifer mostly occurs through recharge from the Sava River, infiltration from precipitation, recharge from leaky water supply and sewerage network, by water inflow through the western boundary from the adjacent Samobor-Zaprešić aquifer and by water inflow through the southern boundary from the Vukomeričke Gorice hills. Infiltration from precipitation, as one of the main recharge components of the Zagreb aquifer, is more closely studied as a part of this research. Soil moisture content is the water contained in the unsaturated soil area and controls the amount of precipitation infiltration, groundwater recharge, evapotranspiration and crop growth. Numerous soil moisture measurement methods exist, for example Time Domain Reflectometry (TDR) probes, neutron probes, gamma-ray attenuation, capacitance and frequency domain reflectometry, etc., but the vast majority of them are soil-invasive, time-consuming, or provide only local information at sparse locations. Geophysical mapping of soil moisture can provide information about soil moisture noninvasively and over larger areas. Many authors reported about the connection between geophysical data and soil moisture (LaBrecque et al., 1992; Sheets and Hendrickx, 1995; Archie, 1942; Binley et al., 2002; Looms et al., 2008; de Jong et al., 2020), but there were no straightforward software tools which would facilitate geophysical mapping of soil moisture. Geophysical methods such as direct-current electrical resistivity, electromagnetic induction, nuclear magnetic resonance, ground-penetrating radar, seismic and time-lapse gravity have sensitivity to soil moisture. Electrical conductivity (EC) can be derived from electrical or electromagnetic induction methods, which can provide one-, two- and three-dimensional surveys. Terry et al. (2018) presented *MoisturEC*, a software written in R language, which simplifies the translation of EC data into soil moisture data and enables filling in the blanks between measurement locations. In this research, the *MoisturEC* program is used to obtain 2D soil moisture profiles of the unsaturated zone in the area of the Velika Gorica well field. Input data consisted of EC data derived from electrical resistivity measurements, point moisture data measured with TDR probes, and calibration file containing EC and moisture data measured with TDR probes as well. Electrical resistivity data were obtained from a 2D geophysical survey using the electrical resistivity tomography method. Moisture content distribution at the observed 2D unsaturated zone profile represents an initial condition in the unsaturated flow model and therefore represents a valuable model input variable.

2. Study area

The study site is located in the southern part of the Zagreb aquifer (Fig. 1) where a research polygon is constructed at the Velika Gorica well field, in order to observe and measure processes in the unsaturated zone.

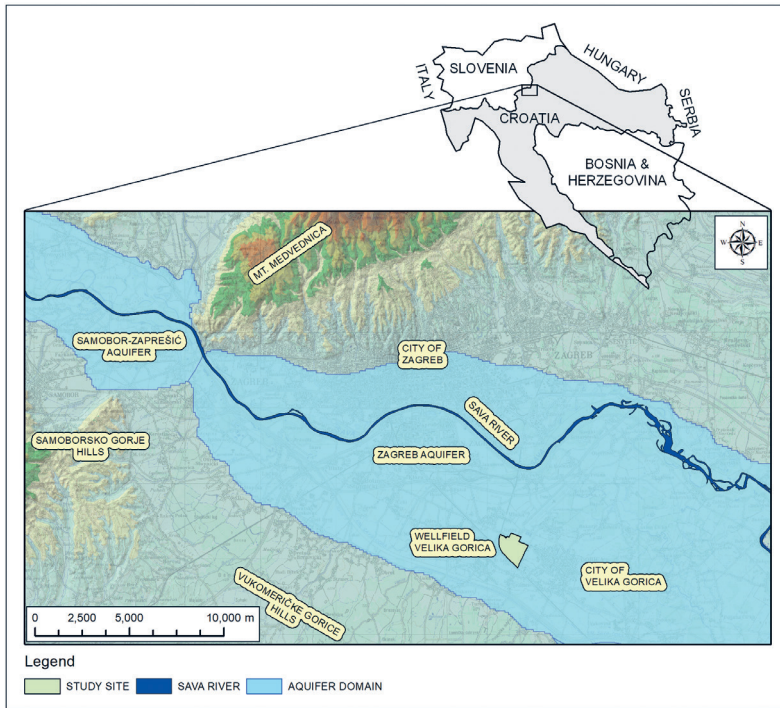


Figure 1. Location of the study area within the Zagreb aquifer domain.

Zagreb aquifer is composed mainly of Quaternary sediments. During the Pleistocene, this area was covered with lakes and marshes. Neighboring mountains (Mt. Medvednica, Vukomeričke gorice hills, Samoborsko gorje hills) were susceptible to intensive erosion. This weathered material was carried along streams and deposited in lakes and marshes at the beginning of the Holocene. Climate and tectonic processes enabled the river Sava to cut its course transporting material from the Alps (Velić and Durn, 1993; Velić et al., 1999). Intensities varied due to climate conditions, with high intensities during warm and wet periods and reduced intensities during dry and cold periods. The consequence of such deposition conditions was pronounced heterogeneity and anisotropy of the aquifer sediments as well as unequal distribution of the aquifer thicknesses. The composition of the lower Pleistocene deposits is predominantly yellowish-red, yellowish-orange, and yellowish-brown, clayey silts/silty clays with sporadic lenses and interbeds of gravelly-sands. The lower and middle part of the Middle Pleistocene unit is predominantly composed of grey-colored sands while the upper part comprises grey-colored or red to yellowish-brown mottled silt and clay-sized material (Velić and Durn, 1993). Frequent lateral changes of gravels, sands, silts, and clays occur in the Upper Pleistocene unit. The Holocene is composed

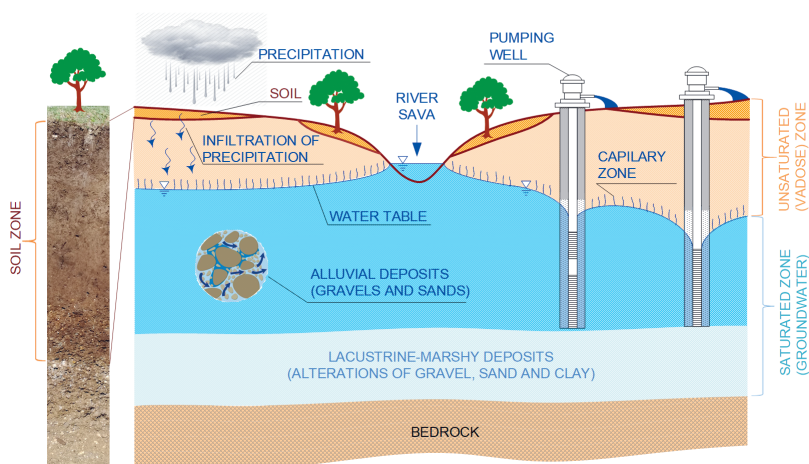


Figure 2. Schematic hydrogeological cross-section of Zagreb aquifer.

of pale, yellowish-grey colored gravels and sands in which limestone cobbles prevail. Quaternary deposits are divided into three basic units: aquifer system overburden *i.e.* soil zone built of clay and silt, shallow Holocene aquifer built of alluvial deposits *i.e.* medium-grain gravel mixed with sands, and deeper aquifer from Middle and Upper Pleistocene built of lacustrine-marshy deposits, with frequent lateral and vertical alterations of gravel, sand and clay (Fig. 2).

The research polygon consists of a research pit and a weather station where different measuring instruments for unsaturated zone monitoring are installed. The profile encompasses the aquifer system overburden, *i.e.* the soil zone, and the alluvial deposits composed of unsaturated gravels and sands down to the water table, *i.e.* the saturated zone. The thickness of the unsaturated zone at the

Table 1. Granulometric data and TDR probe positions (modified according to Ružičić et al. (2019) and Kukulja (2018)).

Depth (cm)	Gravel (%)	Sand (%)	Silt (%)	Clay (%)	TDR probe	USDA texture class	Total porosity (%)	Bulk density (g/cm ³)
0–15	0.00	18.30	54.83	26.87	TP1	Silt loam	46.70	1.37
15–55	0.00	5.14	55.33	39.53	TP2	Silt clay loam	45.70	1.41
55–90	0.74	12.98	50.75	35.53	TP3	Silt clay loam	39.53	1.59
90–117	52.20	1.50	45.65	0.64	TP4	–	–	–
160	–	–	–	–	TP5	–	–	–
200	60.30	38.90	0.80	–	TP6	–	–	–

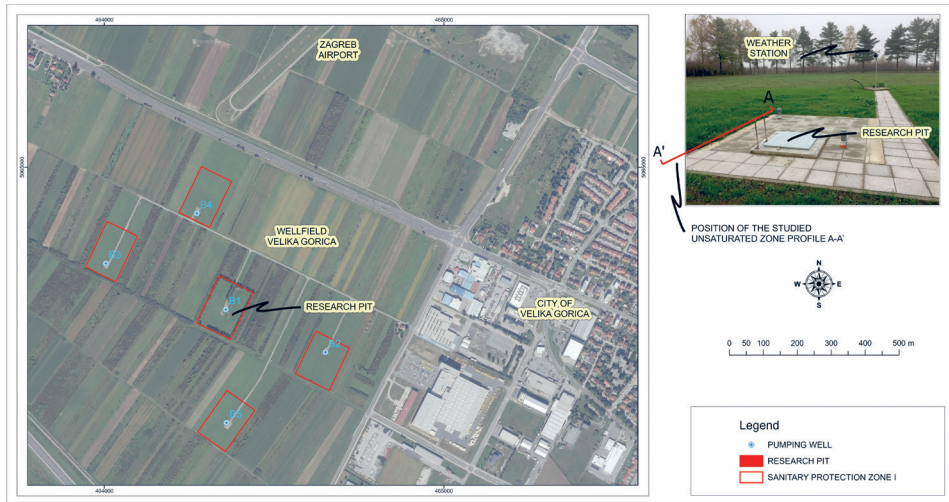


Figure 3. Location of the research polygon.

study site varies between 4.5 and 7.7 meters, depending on the groundwater levels. The wider study area is generally covered by three main pedological units: Fluvisols, Stagnosols, and Eutric Cambisols deposited on Holocene gravels and sands (Ružičić, 2013), while the research polygon itself is situated in Eutric Cambisols deposited on Holocene sediments (Bogunović et al., 1998). According to the United States Department of Agriculture (USDA) soil textural classification, the first 90 centimeters of the observed research pit profile is comprised of silt loam and silt clay loam (Tab. 1), while gravels with sands dominate down to the water table. The studied profile location is covered with grass all season.

The research pit was constructed in the near vicinity of the pumping well B-1 at the Velika Gorica well field (Fig. 3). The Velika Gorica well field has five pumping wells which pump groundwater for the public water supply of the city of Zagreb and the city of Velika Gorica.

3. Materials and methods

3.1. Field measurements

The studied unsaturated zone profile is the eastern wall of the research pit (Figs. 3–5), where TDR probes (IMKO Trime Pico 64) are installed. TDR probes measure hourly moisture content, and EC and the measurements are saved to the Datalogger DT80 and GlobeLog (IMKO) data loggers. TDR probes are situated at the following depths: –10 cm, –35 cm, –74 cm, –100 cm, –160 cm and –200 cm (Tabs. 1 and 2, Fig. 4). The observed unsaturated zone profile is 300 centimeters long and 300 centimeters deep. A-A' 2D profile has dimensions

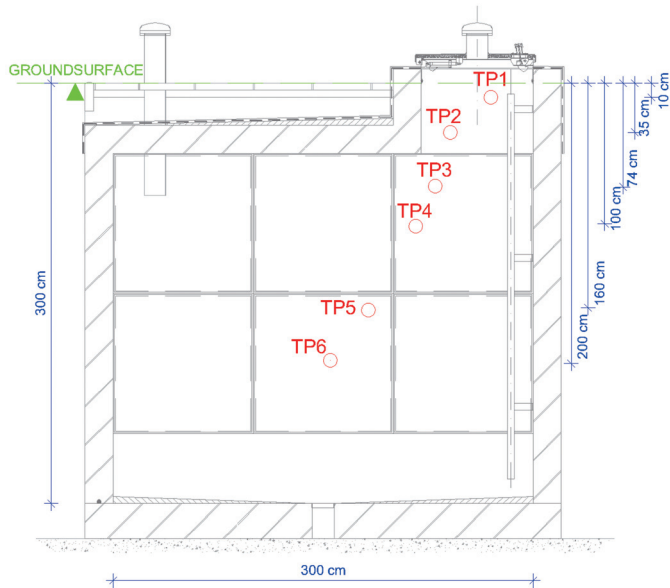


Figure 4. Research pit design and TDR probe positions.

300 cm × 300 cm because it represents the geometry of future numerical water flow model through the unsaturated zone.

In order to establish the initial distribution of soil moisture in the unsaturated zone, TDR probes were installed along with the observed unsaturated profile at different depths. TDR method is an electromagnetic method that de-



Figure 5. Eastern wall of the research pit with installed TDR probes (TP1 to TP6) – view from inside.



Figure 6. Location of the geophysical profile and the research pit.

termines the propagation velocity of a voltage pulse sent into the soil through the probe’s metallic rod. The voltage pulse propagates as an electromagnetic wave. The propagation velocity is calculated from the travel time of the voltage pulse and the length of the probe (Topp and Reynolds, 1998). The velocity of the pulse changes with the change of soil moisture content due to the relatively large dielectric value of water compared to the small dielectric value of solid materials (Malicki et al., 1992).

The geophysical survey took place on November 8, 2019. The method used was the electrical resistivity tomography method, which is frequently used in

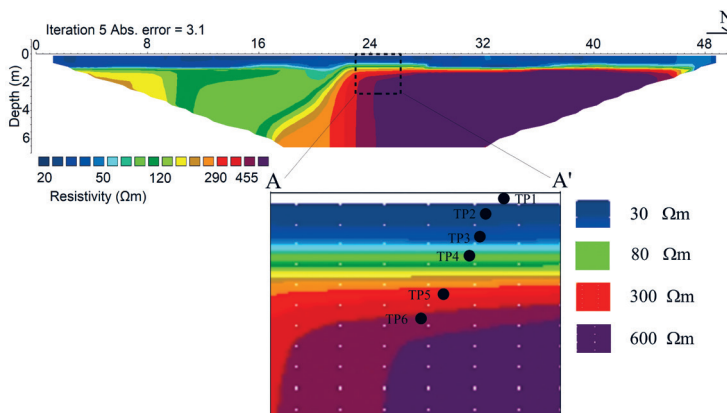


Figure 7. The inverse resistivity model and magnified section of the observed A-A' profile.

shallow hydrogeological, geotechnical, and other research (Šumanovac and Weisser, 2001; Šumanovac, 2006). Electrical resistivity measurements were performed using the Terrameter SAS 1000 and the automatic multielectrode system LIS (Lund Imaging System) from the Swedish company ABEM. The electrodes were arranged in a 50 meter long profile using a Wenner array at 0.5 m unit electrode spacing. The studied unsaturated zone profile (A-A') is situated in the middle of the geophysical profile, approximately at a distance of 25 m (Figs. 6 and 7). Electrical resistivity tomography data are interpreted using Res2dInv geoelectrical inversion software (Loke and Berker, 1995,1996). The data converged within five iterations and the measure of fit between inverted and measured data is 3.1%.

3.2. *MoisturEC*

MoisturEC is a software written in R (R Core Team, 2017) with a graphical user interface that combines EC data from geophysical measurements, point moisture measurements from the field, and optional inputs of calibration and resolution data in order to convert EC data to moisture through a petrophysical transform function (Terry et al., 2018). The final result of moisture estimates is an optimal trade-off between data fit and smoothing. Users can choose between three options of translating EC data into soil moisture. All three options have two mandatory input data – EC and point moisture, in the form of Comma Separated Values (.CSV) files containing coordinate information, data values, and percent error in five columns. EC values must be in S/m and point moisture values must be in fractional values.

The first option allows users to perform a rearranged Archie's law equation:

$$\theta = \varnothing \left(\frac{\sigma_b}{(\varnothing_{int})^m \sigma_\omega} \right)^{1/n}, \quad (1)$$

where θ is moisture content (–), \varnothing is total porosity (–), σ_b is bulk conductivity of soil (S/m), \varnothing_{int} is effective porosity (–), σ_ω – pore fluid conductivity (S/m), m is cementation factor related to pore geometry (–) and n is exponent describing the variation in the conductivity of material due to the water content in pores (–).

In addition to point moisture values and EC values, the user also must enter values of Archie parameters listed above. In practice, the information on most of the parameters in Eq. (1) is usually not available or limited. Therefore, the program offers the second option that allows the user to enter a CSV calibration file containing EC values and moisture content values that form a relationship. These values can be obtained, for example, through a wetting experiment using a soil sample from the site of interest. MoisturEC estimates the parameters through a linear regression:

$$\ln(\theta) = \ln(x) + \frac{\ln \sigma_b}{n}, \quad (2)$$

where x is $x = \left(\frac{\phi}{(\phi_{int}) m_{\sigma_o}} \right)^{1/n}$

and therefore,

$$\theta = x \sigma_b^{1/n}. \quad (3)$$

There is also a third option, where MoisturEC processes the data using Eq. (2). Here the program uses point moisture information and finds the nearest (spatially) EC values to calculate the parameters of Eq. (2).

Moisture content in grid nodes m are estimated through a linear solution of the equation:

$$[J^T C_D^{-1} + \alpha D^T D] m = J^T C_D^{-1} d \quad (4)$$

where d is a column vector of all moisture data and it consists of combined point moisture and EC-derived estimates of moisture content, J is the Jacobian matrix (in this case J consists of ones in the rows and columns that correspond to the nearest grid point in which data are available; elsewhere zero), C_D is a diagonal covariance matrix which consists of the measurement error variances e (and C_D^{-1} are the data weights), D is regularization matrix consisting of a first derivative finite-difference filter between adjacent model elements, and α is the tradeoff parameter that controls the balance between regularization criteria and data misfit. Larger values for α promote an increasingly flat solution. For the first estimate, α is set to 1 (equal trade between smoothing and data misfit). The trade-off value is then repeatedly perturbed to find an optimum value for α to compute the final set of model parameters m . Optimum α value means that the data misfit between the data itself (EC-derived moisture and point moisture) and the linear solution of Eq. (4) is in the order of magnitude of the estimated input errors, which include data errors and Archie or calibration parameter errors.

4. Results and discussion

A geophysical survey at the research location was performed in order to obtain the distribution of electrical resistivity values of the observed soil profile A-A'. Small electrode spacing (0.5 m), and near-surface study area are favorable for determining the true resistivity since the pseudosection is dominated by the near-surface structure. Figure 7 displays electrical resistivity data of 50 m long profile and magnified section with the position of A-A' profile and TDR probes. In the near-surface zone of the entire profile, resistivity is low (< 50 Ω m). The

thickness of this near-surface layer of silt/silty clay varies and is generally between 1 and 2 m (Tab. 1). At a depth of about 2 m, resistivity increases, indicating a sandy-gravelly layer. Lateral changes in resistivity of this layer indicate significant changes in granulometric composition, and the highest resistivities are detected at and near the location of the research pit. The resistivity of these deposits is $> 300 \Omega\text{m}$ and goes beyond $600 \Omega\text{m}$, indicating dry gravels above the groundwater level which show moisture content of around 6% (Tab. 2). The sharp resistivity transition in the second half of the profile relates to the transition from silty and clayey material to the unsaturated gravelly and sandy sediments, which is consistent with the granulometric data in Tab. 1. Given the marked heterogeneity of the Zagreb aquifer, sudden lateral and vertical changes in granulometric composition are a common occurrence.

The measurements of moisture content obtained by TDR probes on November 8, 2019, at 11 a.m. are presented in Tab. 2. Along with geophysical data, they are mandatory input data for the MoisturEC program. The measurement time corresponds to the geophysical survey time (November 8, 2019, 11 a.m.).

All three possible options in the MoisturEC program were tested. In the option where the calibration file is used, 6 different calibration files obtained from 6 different TDR probes were tested. Our calibration curves presented in Fig. 8 were obtained under natural conditions, *i.e.*, they represent raw field data of EC and moisture content, unlike calibration curves obtained from an induced wetting experiment, as suggested by Terry et al. (2018). As hourly measurements of moisture content and EC were available in each of the 6 TDR probes, several calibration curves (from different measurement periods) for each probe were considered, and the most representative ones were used in the MoisturEC program. Moisture content and EC calibration data used in MoisturEC are presented in Fig. 8.

The results of the moisture content distribution θ (–) along the observed A-A' profile obtained by the MoisturEC program using different calibration curves are presented in Fig. 9. White circles indicate TDR probe positions. For calibration data from the TP1 probe (Fig. 9a), moisture content values in the top 90 cm of unsaturated zone profile, where silty and clayey materials dominate, vary between 30 and 50%. These values are realistic, and they are the best fit for the

Table 2. EC and moisture content values measured by TDR probes on November 8, 2019, 11 a.m. with depths (y) and distances (x) along A-A' profile.

TDR probe position	TP1 $y = -0.1 \text{ m}$ $x = 25.77 \text{ m}$	TP2 $y = -0.35 \text{ m}$ $x = 25.48 \text{ m}$	TP3 $y = -0.74 \text{ m}$ $x = 25.37 \text{ m}$	TP4 $y = -1 \text{ m}$ $x = 25.23 \text{ m}$	TP5 $y = -1.6 \text{ m}$ $x = 24.9 \text{ m}$	TP6 $y = -2 \text{ m}$ $x = 24.63 \text{ m}$
Electric conductivity (S/m)	0.0372	0.0399	0.0216	0.0264	0.0217	0.0164
Moisture content (–)	0.407	0.394	0.363	0.246	0.095	0.059

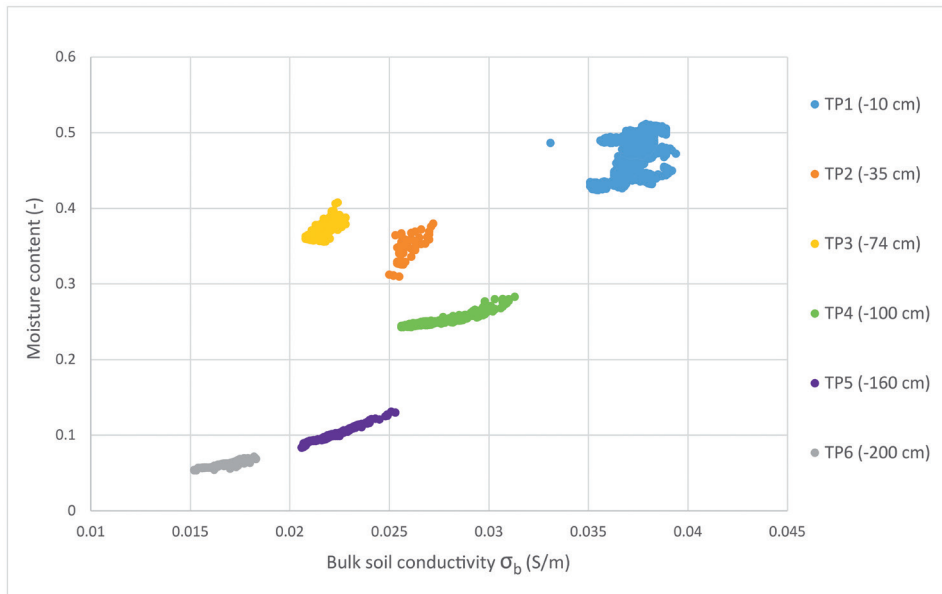


Figure 8. Calibration data used in the MoisturEC program.

measured moisture content values in the field for all TDR probes (Tab. 2). Moisture content values in gravelly material that can be found at depths below -160 cm are less than 15%, which also correspond to TDR measurements displayed in Tab. 2. Moisture content values around -100 cm depth, where the TP4 probe is located, are 20% or less, which is somewhat lower than expected, *i.e.* 24%. With calibration data from the TP2 probe (Fig. 9b), MoisturEC didn't obtain realistic results except for small yellow areas around -35 cm depth where moisture content values are around 37%. For the rest of A-A' profile area moisture content values are too low (17% at -10 cm depth and less than 5% below 90 cm depth). Very similar results were obtained using TP5 calibration data (Fig. 9e), only here moisture content values are found to be even lower at a depth of -10 cm, and amounted to around 12%. With calibration data from the TP3 probe (Fig. 9c), moisture content values mostly correspond to values presented in Tab. 2, except for light green areas around -35 cm depth where moisture content values are too high (around 65%) compared to Tab. 2. Moisture content values obtained by calibration file from TP4 probe (Fig. 9d) showed too low moisture values for the profile part above -150 cm depth compared to the values in Tab. 2. Figure 9f presents moisture content values obtained by calibration file from the TP6 probe, and they are too low for the whole A-A' profile area compared to the measured values presented in Tab. 2. Questionable MoisturEC results of moisture content distribution presented in Figs. 9b-f may indicate that the calibration curves are not suitable input data in the case when they cover a small

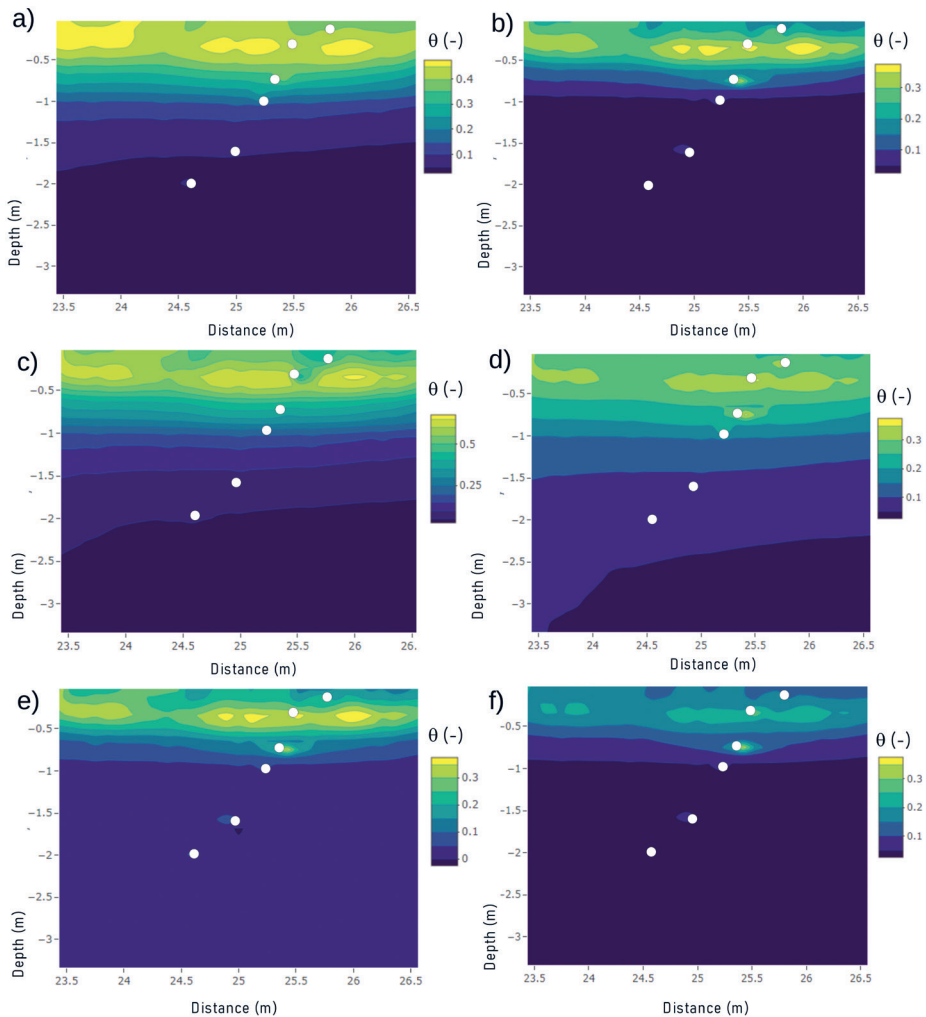


Figure 9. MoisturEC results of moisture content distribution along A-A' profile obtained by using calibration data from: *a)* TP1 probe, *b)* TP2 probe, *c)* TP3 probe, *d)* TP4 probe, *e)* TP5 probe, and *f)* TP6 probe. White circles indicate TDR probe positions listed in Tab. 2.

range of moisture content values (less than 10%). Therefore, the conclusion was made that the calibration data from the TP1 probe (Fig. 9a) can be used as the best fit if we use the calibration curve as input data for the MoisturEC program.

Apart from using calibration curves to obtain moisture content values on A-A' profile, the remaining two options of the MoisturEC program were tested, including only geophysical data and point moisture data as input data. Figure 10a presents moisture content distribution on A-A' profile obtained by using the

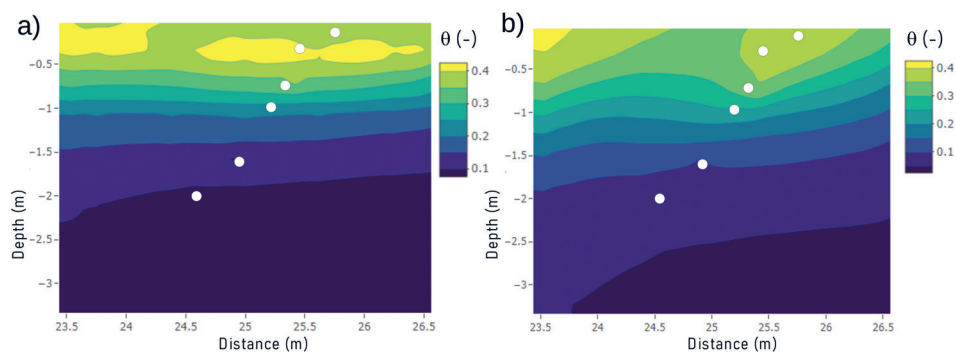


Figure 10. MoisturEC results of moisture content distribution along A-A' profile obtained by *a)* using rearranged Archie's law equation and *b)* by using only point moisture data measured by TDR probes and EC data from the geo-physical survey. White circles indicate TDR probe positions listed in Tab. 2.

rearranged Archie's law. Archie parameters were: $\emptyset = 0.3$, $\emptyset_{int} = 0.2$, $\alpha = 0.5$, $m = 2$, $n = 2$. The resulting moisture content values on A-A' profile fully correspond to the measured values displayed in Tab. 2 at all depths. Finally, Fig. 10b shows moisture content values in the case when MoisturEC uses point moisture information and finds the nearest (spatially) EC values in order to calculate the parameters of Eq. (2). The lateral distribution of moisture content is somewhat different from all previous MoisturEC results, but in most areas of the profile, moisture content values are consistent with values in Tab. 2. The largest difference between measured and calculated values can be seen at the depth of -74 cm, where moisture content is calculated as 23%, which is 13% lower than the actual measured value of 36%. Briefly, the results presented in Fig. 10 suggest that the MoisturEC program provides reasonable results in case when the calibration curves are not available.

5. Conclusions

Geophysical methods have a great potential to advance the mapping of soil moisture and thereby improve groundwater management. In this research, the MoisturEC program is used to provide moisture content distribution at the observed 2D unsaturated zone profile located at Velika Gorica well field site, Zagreb aquifer, based on electrical resistivity tomography measurements and measurements provided by the TDR probes. Mandatory input data consist of inverse values of electrical resistivity data and point moisture data. Optionally, the user can enter a calibration file containing EC and moisture content data of a specific soil sample. MoisturEC program offers three options of translation EC to a moisture content which are all tested in this research. When the calibration curves option was used, realistic moisture content distribution results along the

observed profile were obtained using the calibration curve for the TP1 probe. As for the remaining 5 TDR probes, the resulting moisture content distributions along the observed profile are not convincing given the measured values obtained by TDR probes. A possible cause of such results may be that the calibration curves don't cover a sufficiently large range of moisture content values for a specific soil or sediment. Therefore, if calibration curves are used as input data, it is preferable to conduct a saturation experiment for the soil of interest, as suggested by Terry et al. (2018). However, if calibration curves aren't available, MoisturEC can provide reasonable results that are consistent with the measured data in the research pit with input data from geophysical measurements and TDR probe measurements only. Moisture content distribution at the unsaturated zone profile represents an initial condition for the unsaturated flow model and therefore represents a valuable model input variable.

Acknowledgments – The equipment installed at the research polygon at Velika Gorica well field site was funded by the University of Zagreb.

The research polygon was designed and built with the financial support of VG Vodopskrba d.o.o.

References

- Archie, G. E. (1942): The electrical resistivity log as an aid in determining some reservoir characteristics, *Soc. Petrol. Eng. J.*, **146**, 52–64, <https://doi.org/10.2118/942054-G>.
- Binley, A., Winship, P., Jared West, L., Pokar, M. and Middleton, R. (2002): Seasonal variation of moisture content in unsaturated sandstone inferred from borehole radar and resistivity profiles, *J. Hydrol.*, **267**, 160–172, [https://doi.org/10.1016/S0022-1694\(02\)00147-6](https://doi.org/10.1016/S0022-1694(02)00147-6).
- Bogunović, M., Vidaček, Ž., Racz, Z., Husnjak, S. and Sraka, M. (1998): Inventory of soils in Croatia, *Agriculturae Conspectus Scientificus*, **63**(3), 105–112.
- de Jong, S. M., Heijnen, R., A., Nijland, W. and van der Meijde, M. (2020): Monitoring soil moisture dynamics using electrical resistivity tomography under homogeneous field conditions, *Sensors*, **20**, 1–18, <https://doi.org/10.3390/s20185313>.
- Kukulja, A. (2018): Određivanje hidrauličke vodljivosti metodom permeametra sa stalnom razinom na području Velike Gorice (*Determination of hydraulic conductivity using constant head permeability test method in the area of well field Velika Gorica*). Unpubl. Master's Thesis, Faculty of Mining, Geology and Petroleum Engineering, University of Zagreb, 39 p (in Croatian).
- LaBrecque, D. J., Daily, W. D., Ramirez, A. and Nitao, J. (1992): Electrical resistivity tomography of vadose water movement, *Water Resour. Res.*, **28**, 1429–1442, <https://doi.org/10.1029/91WR03087>.
- Loke, M. H. and Barker, R. D. (1995): Improvements to the Zohdy method for the inversion of resistivity sounding and pseudosection data, *Comput. Geosci.*, **21**, 321–332, [https://doi.org/10.1016/0098-3004\(94\)00075-6](https://doi.org/10.1016/0098-3004(94)00075-6).
- Loke, M. H. and Barker, R. D. (1996): Practical techniques for 3-D resistivity surveys and data inversion, *Geophys. Prospect.*, **44**, 449–523, <https://doi.org/10.1111/j.1365-2478.1996.tb00162.x>.
- Looms, M., C., Jensen, K. H., Binley, A. and Nielsen, L. (2008): Monitoring unsaturated flow and transport using cross-borehole geophysical methods, *Vadose Zone Journal*, **7**, 227–237, <https://doi.org/10.2136/vzj2006.0129>.
- Malicki, M. A., Plagge, R., Renger, M. and Walczak, R. T. (1992): Application of time-domain reflectometry (TDR) soil moisture miniprobe for the determination of unsaturated soil water characteristics from undisturbed soil cores, *Irrig. Sci.*, **13**, 65–72, <https://doi.org/10.1007/BF00193982>.

- Posavec, K. (2006): Identifikacija i prognoza minimalnih razina podzemne vode zagrebačkog aluvijalnog vodonosnika modelima recesijskih krivulja (*Identification and prediction of minimum ground water levels of Zagreb alluvial aquifer using recession curve models*). Unpubl. PhD Thesis, Faculty of Mining, Geology and Petroleum Engineering, University of Zagreb, 89 p (in Croatian).
- R Core Team (2017): *R: A language and environment for statistical computing*. Vienna, Austria: R Foundation for Statistical Computing.
- Ružičić, S. (2013): Model transporta potencijalno toksičnih elemenata kroz nesaturiranu zonu na području regionalnoga vodocrpilišta Kosnica (*Transport model of potentially toxic elements through unsaturated zone at regional well field Kosnica*). Unpubl. PhD Thesis, Faculty of Mining, Geology and Petroleum Engineering, University of Zagreb, 147 p (in Croatian).
- Ružičić, S., Kovač, Z., Perković, D., Bačani, L. and Majhen, Lj. (2019): The relationship between the physicochemical properties and permeability of the fluvisols and eutric cambisols in the Zagreb aquifer, Croatia, *Geosciences*, **9**(10), 1–19, <https://doi.org/10.3390/geosciences9100416>.
- Sheets, K. R. and Hendrickx, J. M. H. (1995): Noninvasive soil water content measurement using electromagnetic induction, *Water Resour. Res.*, **31**(10), 2401–2409, <https://doi.org/10.1029/95WR01949>.
- Šumanovac, F. (2006): Mapping of thin sandy aquifers by using high resolution reflection seismics and 2-D electrical tomography, *J. Appl. Geophys.*, **58**, 144–157, <https://doi.org/10.1016/j.jappgeo.2005.06.005>.
- Šumanovac, F. (2006): Erratum to Mapping of thin sandy aquifers by using high resolution reflection seismics and 2-D electrical tomography, *J. Appl. Geophys.*, **59**, 345–346, <https://doi.org/10.1016/j.jappgeo.2005.04.005>.
- Šumanovac, F. and Weisser, M. (2001): Evaluation of resistivity and seismic methods for hydrogeological mapping in karst terrains, *J. Appl. Geophys.*, **47**, 13–28, [https://doi.org/10.1016/S0926-9851\(01\)00044-1](https://doi.org/10.1016/S0926-9851(01)00044-1).
- Terry, N., Day-Lewis, F. D., Werkema, D. and Lane Jr, J. W. (2018): MoisturEC: A new R program for moisture content estimation from electrical conductivity data, *Groundwater*, **56**, 5, 823–831, <https://doi.org/10.1111/gwat.12650>.
- Topp, G. C. and Reynolds, W. D. (1998): Time domain reflectometry: technique for measuring mass and energy in soil, *Soil Tillage Res.*, **47**, 125–132, [https://doi.org/10.1016/S0167-1987\(98\)00083-X](https://doi.org/10.1016/S0167-1987(98)00083-X).
- Velić, J. and Durn, G. (1993): Alternating lacustrine-marsh sedimentation and subaerial exposure phases during quaternary: Prečko, Zagreb, Croatia, *Geol. Croat.*, **46**, 71–90.
- Velić, J., Saftić, B. and Malvić, T. (1999): Lithologic composition and stratigraphy of quaternary sediments in the area of the “Jakuševac” waste depository (Zagreb, Northern Croatia), *Geol. Croat.*, **52**, 119–130.
- Vujević, M. and Posavec, K. (2018): Identification of groundwater level decline in the Zagreb and Samobor-Zapresic aquifers since the sixties of the twentieth century, *Rud.-geol.-naft. Zb.*, **33**(4), <https://doi.org/10.17794/rgn.2018.4.5>.

SAŽETAK

Određivanje sadržaja vode u tlu pomoću rezultata geofizičkih istraživanja na području vodocrpilišta Velika Gorica, zagrebački vodonosnik

Laura Bačani, Kristijan Posavec, Franjo Šumanovac i Josipa Kapuralić

Poznavanje raspodjele vlažnosti u nesaturiranoj zoni može doprinijeti razumijevanju toka vode kroz nesaturiranu zonu a time i omogućiti izračun prihranjivanja vodonosnika putem oborine. Jedan dio prihranjivanja zagrebačkog vodonosnika čini oborina. U

cilju promatranja i modeliranja infiltracije oborine kroz nesaturiranu zonu izgrađen je znanstveno-istraživački poligon na vodocrpilištu Velika Gorica, u južnom dijelu zagrebačkog vodonosnika, u kojem postoje satna mjerenja električne vodljivosti i sadržaja vode u tlu. Električna vodljivost i vlažnost mjere se TDR (eng. Time Domain Reflectometry) sondama koje su postavljene na različitim dubinama u nesaturiranoj zoni. Nadalje, provedena su i geofizička mjerenja gdje je korištena metoda električne tomografije. Podaci dobiveni geofizičkim istraživanjem te podaci o električnoj vodljivosti i vlažnosti dobiveni mjerenjima u TDR sondama korišteni su kao ulazni podaci za MoisturEC program u cilju dobivanja raspodjele vlažnosti na promatranom 2D profilu. U ovom istraživanju su testirane tri opcije MoisturEC programa za prevođenje podataka o električnim vodljivostima u podatke o sadržaju vode. Ukupno je dobiveno osam raspodjela vlažnosti po promatranom profilu te se može zaključiti da MoisturEC program daje razumne rezultate u slučaju kada su dostupni ulazni podaci o električnim vodljivostima na promatranom profilu te točkasti podaci o sadržaju vlage iz TDR sonde. Raspodjela vlažnosti u nesaturiranoj zoni može poslužiti kao početni uvjet pri modeliranju toka vode u nesaturiranoj zoni. Razumijevanje toka vode u nesaturiranoj zoni omogućava kvantifikaciju efektivne infiltracije, a time i bolje upravljanje podzemnim vodama.

Ključne riječi: nesaturirana zona, sadržaj vode u tlu, TDR metoda, električna otpornost, zagrebački vodonosnik, MoisturEC program

Corresponding author's address: Laura Bačani, Faculty of Mining, Geology and Petroleum Engineering, University of Zagreb, Pierottijeva 6, 10000 Zagreb, Croatia; e-mail: laura.bacani@rgn.unizg.hr



This work is licensed under a Creative Commons Attribution-NonCommercial 4.0 International License.